



Letter

Hydrogen accommodation in Zr second phase particles: Implications for H pick-up and hydriding of Zircaloy-2 and Zircaloy-4

P.A. Burr^{a,b}, S.T. Murphy^a, S.C. Lumley^{a,c}, M.R. Wenman^{a,*}, R.W. Grimes^a

^a Centre for Nuclear Engineering and Department of Materials, Imperial College London, London SW7 2AZ, UK

^b Institute of Materials Engineering, Australian Nuclear Science & Technology Organisation, Menai, New South Wales 2234, Australia

^c Nuclear Department, Defence Academy, HMS Sultan, Gosport, Hampshire PO12 3BY, UK

ARTICLE INFO

Article history:

Available online 7 December 2012

Keywords:

A. Zirconium
A. Intermetallics
C. Hydrogen absorption

ABSTRACT

Ab-initio computer simulations have been used to predict the energies associated with the accommodation of H atoms at interstitial sites in α , β -Zr and Zr–M intermetallics formed with common alloying additions (M = Cr, Fe, Ni). Intermetallics that relate to the $Zr_2(Ni,Fe)$ second phase particles (SPPs) found in Zircaloy-2 exhibit favourable solution enthalpies for H. The intermetallic phases that relate to the $Zr(Cr,Fe)_2$ SPPs, found predominantly in Zircaloy-4, do not offer favourable sites for interstitial H. It is proposed that $Zr(Cr,Fe)_2$ particles may act as bridges for the migration of H through the oxide layer, whilst the $Zr_2(Ni,Fe)$ -type particles will trap the migrating H until these are dissolved or fully oxidised.

© 2012 Elsevier Ltd. All rights reserved.

1. Introduction

For the past five decades, Sn-containing Zr alloys, such as Zircalloys, have been widely used for nuclear fuel cladding and internal components of light water nuclear reactors [1]. To improve the corrosion resistance, Zircaloy-2 (or Zry-2) also contains small amounts of Fe, Cr and Ni, which precipitate out as SPPs due to their low solid solubility in α -Zr.

Later alloy development led to the formulation of Zry-4, an alloy with much lower Ni content. The reduction of Ni content in Zry-4 resulted in a reduced H pick-up fraction (HPUF) of the alloy without compromising the oxidation resistance [1]. However, the mechanism through which the HPUF is affected by the presence of Ni is still not well understood. There is, nevertheless, general agreement that SPP composition, size and morphology play a key role [2].

There are many theories as to how intermetallics influence corrosion and H pickup but all are subject to challenge [3–7]. Hatano et al. [3] suggested that as the oxide layer thickens, the larger SPPs residing at the oxide–metal interface will oxidise more slowly than the surrounding Zr. These partially metallic particles could then act as a H migration pathway (bridge) through the oxide layer. It has been noted by Shaltiel et al. [8] that Laves-phase SPPs of the $Zr(Fe,Cr)_2$ type have a tendency to absorb H. Furthermore, the ratio of Fe to Cr seems to influence H absorption. As SPPs are irradiated the Fe dissolves out first, therefore the ratio of Fe–Cr will change and concomitantly the capacity for H absorption. This may lead

to a release of H into the α -Zr matrix phase late in fuel life, which could accelerate hydriding of the cladding. Equally, subsequent annealing of SPPs, heated up during the early stage of dry storage of fuel, could reabsorb H from the matrix into recrystallized SPPs and hence be beneficial in reducing available H for hydride reorientation. At present there is little data regarding which traps for H are most efficient.

In this paper we employed density functional theory (DFT) to calculate the solution enthalpies of H in the various binary intermetallic SPPs and compare these to the solution enthalpies of H in both α and β -Zr phases. The two most common SPPs are the ternary $Zr(Cr,Fe)_2$ (especially in Zry-4) and $Zr_2(Fe,Ni)$ (in Zry-2). Whilst it has been reported that binary phases do not tend to form in Zr alloys [9–11], an investigation of the simple binary systems is important, in the first instance, to understand the role that individual alloying elements play in the interaction between H and the intermetallic phases. Consequently, this allows us to determine which SPPs are likely to behave as described by Hatano's model, if at all.

Cr forms three intermetallic phases with Zr: the cubic α phase and the hexagonal β and γ phases. All three have the same stoichiometric formula $ZrCr_2$ and are all Laves phases, termed *C15*, *C36* and *C14*, respectively (see Table 1 for further details). Even though the stable phase at reactor operating temperature is α - $ZrCr_2$, there have been many reports of both cubic [12–16] and hexagonal [9–11,14–19] structures in Zr alloys, therefore all three have been considered here. Although the Zr–Ni binary system includes numerous intermetallic phases [20], Zr–Ni SPPs tend to be stable as Zr rich phases, in particular tetragonal Zr_2Ni . Fe is found in the $ZrCr_2$ -type SPPs as well as in the Zr_2Ni -type, therefore the *C15*, *C36* and *C14*

* Corresponding author. Tel.: +44 (0) 2075946763.

E-mail address: m.wenman@imperial.ac.uk (M.R. Wenman).

Table 1

Supercells adopted for each of the phases, in terms of the number (p, q, r) of repeats of the basic crystallographic unit cell parameters \mathbf{a} , \mathbf{b} and \mathbf{c} , the total number of non-hydrogen atoms N , the shortest distance d between defect images in Å, as well as the equivalent hydrogen concentration $[H]$ in wt ppm.

Phase	Space group	p	q	r	N	d	$[H]$
α -Zr	$P6_3/mmc$	5	5	3	150	15.6	73.7
β -Zr	$Im\bar{3}m$	4	4	4	128	14.3	86.3
α -ZrCr ₂ C15	$Fd\bar{3}m$	2	2	2	192	14.3	80.7
β -ZrCr ₂ C36	$P6_3/mmc$	2	2	1	96	10.1	161.3
γ -ZrCr ₂ C14	$P6_3/mmc$	2	2	2	96	10.2	161.3
ZrFe ₂ C15	$Fd\bar{3}m$	2	2	2	192	14.1	77.6
ZrFe ₂ C36	$P6_3/mmc$	2	2	1	96	10.0	155.2
ZrFe ₂ C14	$P6_3/mmc$	2	2	2	96	10.0	155.2
Zr ₂ Fe	$I4/mcm$	2	2	2	96	9.8	132.2
Zr ₂ Ni	$I4/mcm$	2	2	2	96	10.5	130.6

ZrFe₂ Laves phase and the Zr₂Fe phase have all been studied. Fig. 1 contains schematic representation of unit cells of each of the intermetallic phases described above.

2. Computational methodology

All DFT simulations were carried out using CASTEP 5.5 [21]. Ultra-soft pseudo potentials with a consistent cut-off energy of 450 eV were used throughout. Previous work by Domain et al. [22] demonstrated that the Generalized Gradient Approximation (GGA) is better suited than the Local Density Approximation to describe the exchange–correlation functional of solid Zr. Therefore, the Perdew, Burke and Ernzerhof (PBE) [23] parametrisation of the GGA was adopted for this study. A high density of \mathbf{k} -points was employed for the integration of the Brillouin Zone, following the Monkhorst–Pack sampling scheme [24]: the distance between sampling points was maintained as close as possible to 0.030 \AA^{-1} and never above 0.035 \AA^{-1} . The fast fourier transform grid was set to be twice as dense as that of the wavefunctions, with a finer grid for augmentation charges scaled by 2.3. Due to the metallic nature of the system, density mixing and Methfessel–Paxton [25] cold smearing of bands were employed with a width of 0.1 eV. Testing was carried out to ensure a convergence of 10^{-3} eV/atom was achieved with respect to all of the above parameters. All calculations were spin polarised and no symmetry operations were enforced.

The energy convergence criterion for self-consistent calculations was set to 1×10^{-6} eV. Similarly robust criteria were imposed for ionic energy minimisation: energy difference $< 1 \times 10^{-5}$ eV, forces on individual atoms $< 0.01 \text{ eV \AA}^{-1}$ and stress component on cell < 0.05 GPa (for constant pressure simulations).

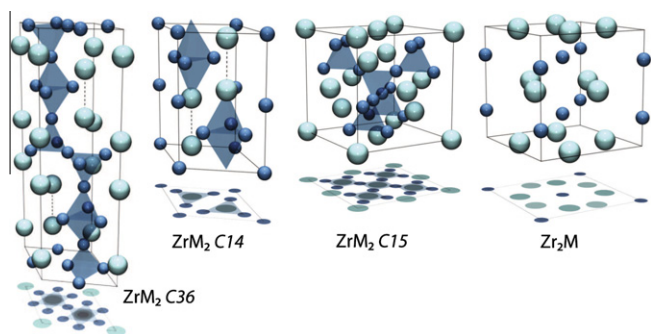


Fig. 1. Unit cells of C36, C14, C15 Laves structure and of Zr₂M. The larger lighter spheres represent the Zr atoms, the smaller darker spheres represent Cr or Fe in the laves phases and Fe or Ni in the Zr-rich phase.

All non-defective structures were relaxed at constant pressure (both the crystal's lattice parameters and ion positions within the supercells were subject to energy minimisation). Relaxed structures were then employed for simulations containing H interstitial defects. Defect simulations were performed both at constant volume (cell parameters constrained to preserve the perfect supercell's shape and volume) and at constant pressure; these replicate dilute and alloying conditions, respectively.

3. Results and discussion

3.1. α and β -Zr

When considering the effective H concentration it is important to bear in mind that the solubility of H in α -Zr is 50–60 wt ppm at the operating temperature of a pressurised water reactor of 300 °C [26,27]. For α -Zr, calculations with a simple H interstitial defect were performed for supercells containing up to 150 atoms ($5 \times 5 \times 3$); yielding an effective defect concentration of 73.7 wt ppm H, therefore only slightly above the reported solubility limit. For β -Zr the solubility limit of H is orders of magnitude larger [26].

The lattice parameters and enthalpy of formation of each phase investigated were presented in previous work [28] and are in agreement with values available in the literature. In addition, the dissociation energy and dimer length of the H₂ molecule were calculated to be 4.53 eV and 752 pm, respectively, in excellent agreement with experimental values, 4.48 eV and 746 pm [29].

α -Zr presents five sites for interstitial occupancy: a tetrahedral site in Wyckoff position [30] 4f (with $z = \frac{5}{8}$), an octahedral site (2a), an hexahedral site (2d), a basal trigonal site (2b), and a non-basal trigonal site (12k, with $x = \frac{4}{9}$, $z = \frac{5}{12}$)—the latter three were found to be metastable for H occupancy (i.e. upon energy minimisation the H atom relaxes into either the tetrahedral or octahedral sites). β -Zr has stable tetrahedral 12d and octahedral 6b interstitial sites. A trigonal interstitial site also exists (24h, with $y = \frac{1}{3}$), however, this too was found to be unstable for H occupancy.

The enthalpy of solution of an isolated H atom in bulk metal, $E_{\text{H}}^{\text{sol}}$, according to reaction 1, was calculated using Eq. 2,

$$M_{x(s)} + \frac{1}{2}H_{2(g)} \rightarrow M_xH_{(s)} \quad (1)$$

$$E_{\text{H}}^{\text{sol}} = E_{M_xH_{(s)}}^{\text{dft}} - E_{M_{x(s)}}^{\text{dft}} - \frac{1}{2}E_{H_{2(g)}}^{\text{dft}} \quad (2)$$

where M is a metal simulated with a supercell containing x atoms.

The calculated values of solution enthalpies for interstitial H in pure Zr are presented in Table 2, together with reference values from both experimental and other *ab initio* simulations.

In α -Zr, it was found that H exhibits a slight preference of the tetrahedral site over the octahedral site by -0.086 eV, however, given the small energy difference between the two sites, the H interstitial atom will probably occupy both sites at reactor temperatures. Previous studies by Domain et al. [22] record the

Table 2

Enthalpy of solution of H in Zr in eV The value by Domain et al. is from DFT simulations, the others are all experimentally derived from pressure–concentration–temperature studies.

Refs.	α -Zr	β -Zr
Current	−0.464	−0.619
Domain [22]	−0.600	
Yamanaka [31]	−0.424	−0.455
Ells [32]	−0.473	−0.688
Mallett [33]	−0.373	−0.077
Kearns [27]	−0.513 ± 0.09	

Download English Version:

<https://daneshyari.com/en/article/1469234>

Download Persian Version:

<https://daneshyari.com/article/1469234>

[Daneshyari.com](https://daneshyari.com)